Available online at www.sciencedirect.com
ScienceDirect
Journal of Nuclear Materials 375 (2008) 243–251
journal of nuclear materials
www.elsevier.com/locate/jnucmat

Post-irradiation examination of AlFeNi cladded U_3Si_2 fuel plates irradiated under severe conditions

A. Leenaers [a,*], E. Koonen [a], Y. Parthoens [a], P. Lemoine [b], S. Van den Berghe [a]

[a] SCK·CEN, Nuclear Materials Science Institute, Boeretang 200, 2400 Mol, Belgium
[b] Commissariat à l'énergie atomique (CEA), Centre de Saclay, 91191 Gif-sur-Yvette cedex, France

Received 24 August 2007

Abstract

Three full size AlFeNi cladded U_3Si_2 fuel plates were irradiated in the BR2 reactor of the Belgian Nuclear Research Centre (SCK·CEN) under relatively severe, but well defined conditions. The irradiation was part of the qualification campaign for the fuel to be used in the future Jules Horowitz reactor in Cadarache, France. After the irradiation, the fuel plates were submitted to an extensive post-irradiation campaign in the hot cell laboratory of SCK·CEN. The PIE shows that the fuel plates withstood the irradiation successfully, as no detrimental defects have been found. At the cladding surface, a multilayered corrosion oxide film has formed. The U–Al–Si layer resulting from the interaction between the U_3Si_2 fuel and the Al matrix, has been quantified as $U(Al,Si)_{4.6}$. It is found that the composition of the fuel particles is not homogenous; zones of USi and U_3Si_2 are observed and measured. The fission gas-related bubbles generated in both phases show a different morphology. In the USi fuel, the bubbles are small and numerous while in U_3Si_2 the bubbles are larger but there are fewer.

1. Introduction

The Commissariat à l'énergie atomique (CEA) is in the process of qualifying U_3Si_2 fuel as start-up fuel for the Réacteur Jules Horowitz (RJH). As such, the performance of the fuel plates under conditions representative for this reactor, have to be studied.

In a previous campaign [1], two sets of three U_3Si_2 fuel plates with a loading of respectively 5.1 g U/cm^3 and 6.1 g U/cm^3 (35% $^{235}U/U_{total}$) were irradiated under conditions corresponding to the upper boundary limit of the regime at which the RJH reactor is planned to operate. The plates had an AG3-NET (Al–Mg alloy) cladding and were submitted to a maximum mean hot plane heat flux of 520 W/cm^2, resulting in cladding and fuel temperatures of over 200 °C. The irradiation program was stopped after the second cycle because of failure of the fuel plates. At the end of the irradiation, the U_3Si_2 plates showed a maximum burn-up of respectively 29% and 25% ^{235}U. In the ensuing post-irradiation examination (PIE) program, it was found that the failure of the plates was entirely related to the corrosion of the aluminum cladding. The high heat fluxes generated by the fuel had caused cladding temperatures to exceed the limit for corrosion resistance of the AG3-NET alloy (>200 °C), which lead to the creation of thick and porous corrosion layers on the cladding surface. Because of the low thermal conductivity of this layer, temperatures had increased further, which accelerated the corrosion until the cladding failed.

The fuel itself had retained its integrity without any deleterious changes in the physical properties. The high temperature to which the fuel was exposed along with the water ingress after failure, caused the complete consumption of the matrix by the formation of a $U_3Al_7Si_2$ interaction phase and the creation of voids in the former Al matrix [1].

In the irradiation program described in this paper, three full size U_3Si_2 fuel plates with a loading of 4.8 g U_{tot}/cm^3 (19.9% $^{235}U/U_{total}$), were irradiated in the BR2 reactor

* Corresponding author. Tel.: +32 14 333044; fax: +32 14 321216.
E-mail address: aleenaer@sckcen.be (A. Leenaers).

0022-3115/$ - see front matter © 2008 Elsevier B.V. All rights reserved.
doi:10.1016/j.jnucmat.2008.01.013

under relatively severe conditions corresponding to the standard operating limit of the RJH reactor. The objective of the irradiation was to reach an average fuel burn-up of 55% ^{235}U while maintaining a maximum temperature of the outer cladding surface of 140 °C. The fuel plates have an aluminum–iron–nickel (AlFeNi) cladding instead of the AG3-NET material used in the previous campaign. AlFeNi alloys were selected because they are known to have a good resistance against high-purity water corrosion, even at temperatures as high as 315 °C [2].

2. Experimental

2.1. Fuel plates and irradiation history

A standard BR2 element consists of six concentric tubes, each tube being an assembly of three equal, curved UAl_x based fuel plates. For the test irradiation, three U_3Si_2 fuel plates, manufactured by Compagnie pour l'Étude et la Réalisation de Combustibles Atomiques (CERCA), were used to constitute the outer cylinder of a standard BR2 element. The plates have a fissile material density of 4.8 g U_{tot}/cm^3 and an uranium enrichment of 19.9% $^{235}U/U_{total}$. The meat of the fuel plates consists of U_3Si_2 particles dispersed in a pure aluminum matrix and the cladding of the plates is an Al alloy with 1% Fe, 1% Ni and 1% Mg, commonly called AlFeNi.

The fuel element was incorporated in the BR2 reactor during three irradiation cycles of 22.2, 20.5 and 26.1 operating days, respectively. The results of the thermal hydraulic calculations show that the azimuthally averaged heat flux in the hot plane, averaged over all the cycles, for each of the plates was 260, 260 and 247 W/cm^2, respectively, with peak heat fluxes of over 400 W/cm^2. At their end-of-life, the fuel plates have reached an average burn-up of 54% ^{235}U (1.3×10^{21} fissions/cm^3 meat) with peak burn-ups of 87%, 86% and 79% ^{235}U, respectively (resp. 4.95×10^{21}, 4.82×10^{21} and 4.42×10^{21} fissions/cm^3). From the temperature calculations, it was found that the maximum external cladding surface temperature stayed within the range of 120–140 °C. It should be noted that the thickness of the cladding oxide layer developed during irradiation has a major influence on the temperature. The uncertainty on the temperature values is therefore about 10%.

The fuel element was transferred to the hot cell near the BR2 reactor pool for first non-destructive testing (NDT) and dismantling. After dismantling, the three individual plates were transferred to the laboratory for High and Medium Activity for non-destructive and destructive testing on the plates. The PIE was focused on one plate, which had received an average heat flux in the axial hot plane of 260 W/cm^2 and a peak burn-up of 86% or 4.82×10^{21} fissions/cm^3 meat.

2.2. Post-irradiation examination

The oxide layer thickness was measured using an eddy current probe, while gross gamma and gamma spectroscopic measurements were recorded to analyse the burn-up profile and power distribution over the fuel plate. Based on the NDT results, a sample has been cut from the fuel plate (Fig. 1) at the position of the thickest oxide layer and the highest burn-up and power. The sample, which covers 2/3 of the fuel plate width, was embedded in an epoxy resin in such a way that the complete section of the fuel (meat and cladding) can be observed. The mount was polished with SiC paper of successively finer grain size, finishing on cloth with diamond paste of 3 and 1 μm.

Optical microscopy was performed on a Reichert Telatom 3 remote controlled and shielded optical microscope. The Vickers microhardness of the cladding, the U_3Si_2 fuel, the aluminum matrix and the interaction product formed between the fuel and the aluminum in the meat, were obtained through the indentation of the material with a diamond tip using a force F (gf). For scanning electron microscopy (SEM) a shielded JEOL scanning electron microscope type 6310 was used in secondary and backscattered electron mode.

The electronprobe micro analysis (EPMA) was performed on a shielded CAMEBAX-R Microbeam, upgraded with digital image and X-ray acquisition hard- and software. X-ray mappings were recorded to obtain the lateral distribution of several elements (U, Si, Al, Mg, Fe ...), and the elemental composition was measured using wavelength dispersive X-ray analysis (WDX). Prior to each measurement, a calibration was performed using the appropriate standards (Table 1).

It should be noted that microstructural observations are made at several positions on the sample (as indicated with the white dots on Fig. 1), covering more than half the plate width.

X-ray diffraction (XRD) data of the oxide layer is recorded on a Philips X'Pert θ-θ diffractometer equipped with a Cu tube (Cu $K\alpha_{1,2} = 0.1541$ nm), configured in the standard Bragg–Brentano geometry. Scans of the diffraction peaks in the 10°–90° 2θ range were recorded with the X'Celerator, an X-ray area detector based on RTMS (Real Time Multiple Strip) technology.

3. Results

3.1. Cladding behaviour

Fig. 1 shows the 2D distribution of the oxide layer thickness over the fuel plate. A maximum oxide layer thickness of 30–50 μm is found at the highest flux position. It was found that the oxide layer could be removed easily, by wiping the surface with a moist paper cloth. Some of the removed powder was collected and characterized using X-ray diffraction (XRD), to determine which crystalline phases are present in the oxide layer. Analysis of the recorded XRD pattern (Fig. 2) shows that the major constituents of the powder are boehmite AlO(OH) (JCPDS 021–1307), bayerite $Al(OH)_3$ (JCPDS 077–0114) and aluminum (JCPDS 004–0787).

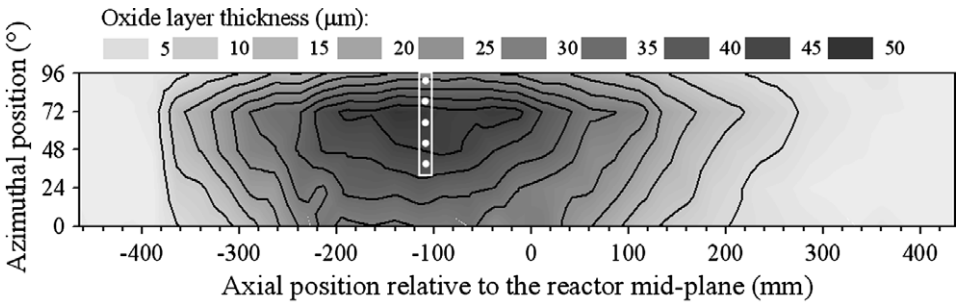

Fig. 1. 3D distribution of the oxide layer of the fuel plate. The white square indicates the size of sample cut from the plate. The white dots are the positions on the sample where microstructural observations are made.

Table 1
Crystals used for X-ray map and quantitative EPMA analysis. Prior to quantification of the elements, calibration is performed using the appropriate standards

Element	X-ray line	Wavelength (pm)	Crystal	Standard
O	Kα	2362.0	PC1	UO_2
Mg	Kα	989.5	TAP	Mg (pure)
Al	Kβ	794.0	TAP	Al_2O_3
Si	Kα	712.7	PET	Si (pure)
Xe	Lα	301.7	PET	Interpolation
Nd	Lα	237.1	LIF	NdF_3
U	Mα	391.0	PET	UO_2

The optical and scanning electron microscopy (Fig. 3(a)) results on the oxide layer all show cracking of the layer and locally even complete detachment from the cladding. This is interpreted as the result of dehydration of the layer (evaporation of the lattice water) during the drying of the fuel element in the hot cell.

Image analysis of the SEM graphs was used to measure the oxide layer thickness. It was found that the thickness of the oxide film on the cladding surface increased from 18 μm at the side of the fuel plate to 55 μm at the center of the fuel plate.

OM and SEM images furthermore show that the cladding contains numerous precipitates, which are identified by reference to the literature [3,4] and X-ray mapping with EPMA, as AlFeNi particles. Due to the high density contrast between the AlFeNi particles and the Al, the backscattered electron image (Fig. 3(b)) clearly shows that the precipitates can also be found in the oxide layer but only in the part of the layer close to the cladding. Closer to the outer surface of the oxide layer, no precipitates are found.

The SEM image on the unpolished outer cladding surface (Fig. 4) clearly shows the cracking of the oxide layer probably due to dehydration. The image of the cross section on the oxide layer of a fractured sample (Fig. 5), shows that the oxide layer consists of two parts. The layer adjacent to the cladding contains precipitates, while the second, thinner layer in contact with the coolant does not show these particles.

The AlFeNi precipitates can also be clearly distinguished in the quantitative linescan covering the cladding and the outer surface oxide layer (Fig. 6). From several measurements on the cladding, an average Fe and Ni content of approximately 1.2 wt% each, 0.8 wt% of magnesium

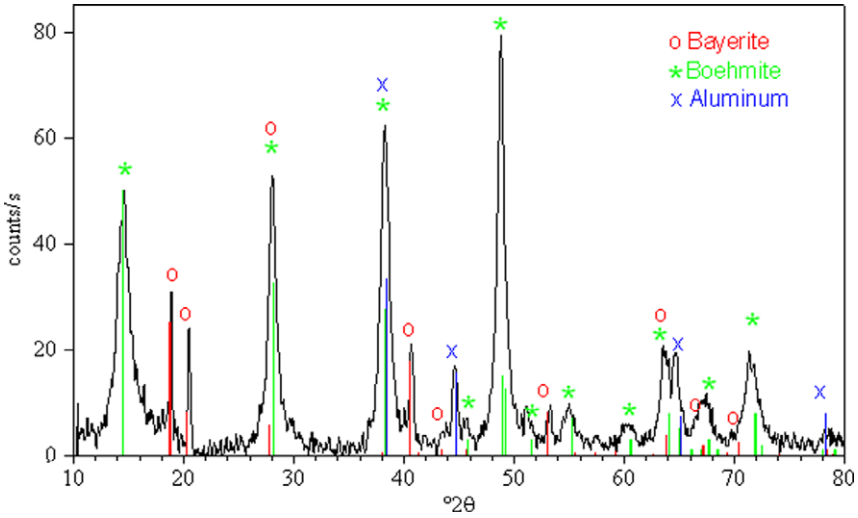

Fig. 2. Measured X-ray diffraction pattern of the oxide layer and the reference pattern JCPDS 021–1307 for boehmite AlO(OH) (∗), JCPDS 077–0114 for bayerite $Al(OH)_3$ (o) and JCPDS 004–0787 for aluminum (×).

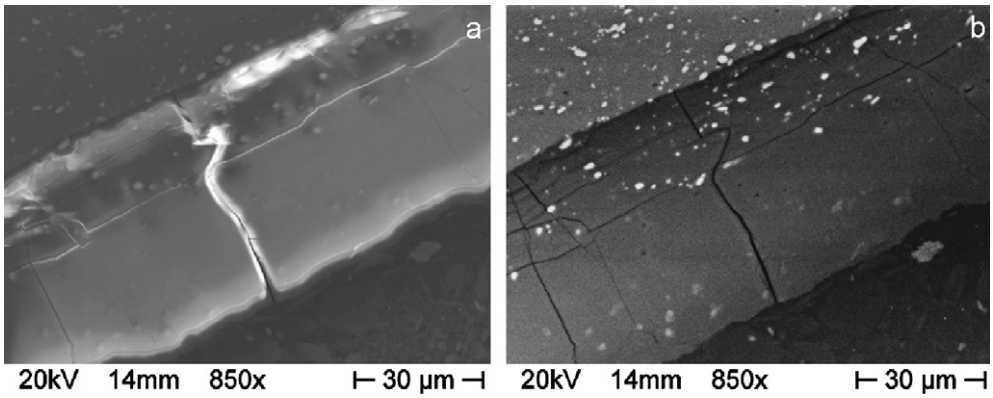

Fig. 3. (a) Secondary electron image showing cracks in the oxide layer. (b) The backscattered electron image of the oxide layer reveals white particles, which are identified as AlFeNi precipitates.

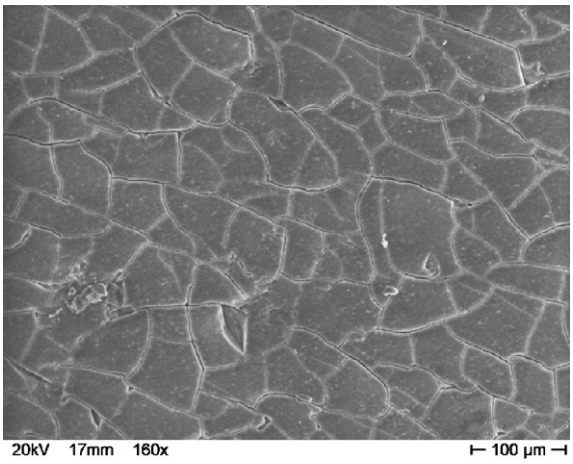

Fig. 4. Secondary electron image of the outer fuel plate surface. The cracked pattern observed is a result of dehydration of the oxide layer.

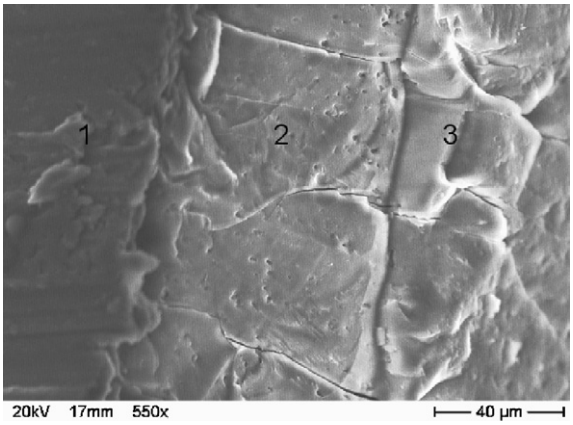

Fig. 5. Secondary electron image of the cladding oxide layer of a fractured sample. The AlFeNi cladding (1) is covered with a double oxide layer of which the one adjacent to the cladding contains precipitates (2) while the outermost layer (3) is thinner and seems not to contain the AlFeNi particles.

and 0.1 wt% of Si is measured, which is in good agreement with the initial composition as given in Table 2.

The Mg X-ray map (Fig. 7), covering the complete section of the fuel, shows that this element is in solid solution in the Al cladding, while the Fe and Ni images illustrate that these elements have indeed formed precipitates.

3.2. Fuel meat behaviour

Even though some oxidation will have occurred in-between the sample preparation and the measuring campaign, it is seen in the oxygen distribution map (Fig. 7) that oxide is present in the fuel particles located at the interface of the meat with the inner and outer cladding. Oxidation of the outer particles of the meat can be related back to the fabrication process and is not uncommon, but should be avoided as it can lead to unbonded areas.

It is observed from the Al map that ample Al matrix is still left within the meat. The uranium and silicon X-ray maps seem to correspond, but areas with increased Si content can be discerned in the Si map.

The main change observed in the meat is the growth of an interaction layer between the fuel particles and the Al matrix (Fig. 8). The thickness of this interaction layer increases from the plate side over the fuel plate width from $\simeq$5 to $\simeq$7 µm.

The local Si X-ray map in Fig. 8 covering a fuel particle within the meat, clearly shows areas with increased Si content within the same particle. In the backscattered electron image, this area has a darker color indicating a less dense structure. This means that there is a difference in fuel composition within the same particle. The zone with the less dense structure (darker zone) is identified as USi (density 10.9 g/cm^3 [5]) while the composition of the remainder of the fuel particle is U_3Si_2 (density 12.2 g/cm^3 [5]). The quantitative linescan (Fig. 9) measured over this fuel particle by EPMA confirms the presence of the two phases.

Looking at the SEM and BSE image (Figs. 8 and 9), in more detail, it is observed that in the USi zone, small fission gas-related bubbles have formed, while in the U_3Si_2 the bubbles have a much larger diameter. This observation is also reflected in the measured xenon content. In the USi

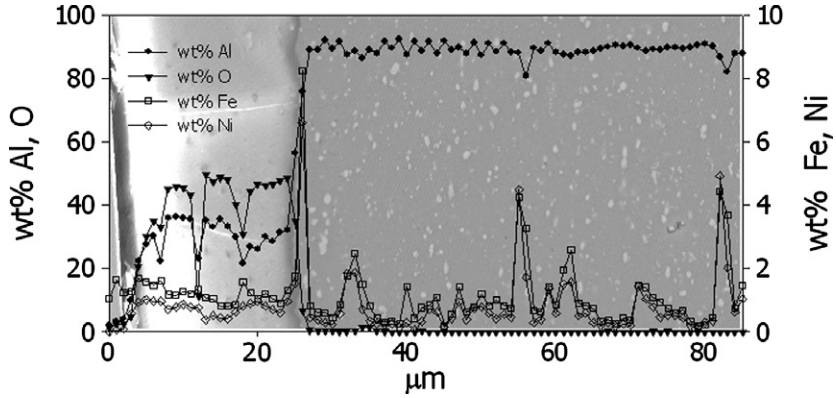

Fig. 6. Quantitative linescan over the cladding at the oxide layer at the surface.

Table 2
Chemical composition of AlFeNi

Element	Concentration specified (wt%)	Concentration measured (wt%)	Element	Concentration specified (wt%)	Concentration measured (wt%)
Fe	0.8–1.2	1.01	Ti	0.02–0.08	0.05
Ni	0.8–1.2	1.02	B	<0.001	0.0002
Fe + Ni	Min. 1.8	2.03	Li	<0.001	0.0005
Mg	0.8–1.2	1.15	Cd	<0.001	0.0001
Cr	0.2–0.5	0.31	Cu	<0.008	0.0026
Mn	0.2–0.6	0.26	Si	<0.3	0.07
Zr	0.06–0.14	0.09	Zn	<0.03	0.006

The measured values are obtained from the quality control certificate No.: C-65–4666 by CERCA.

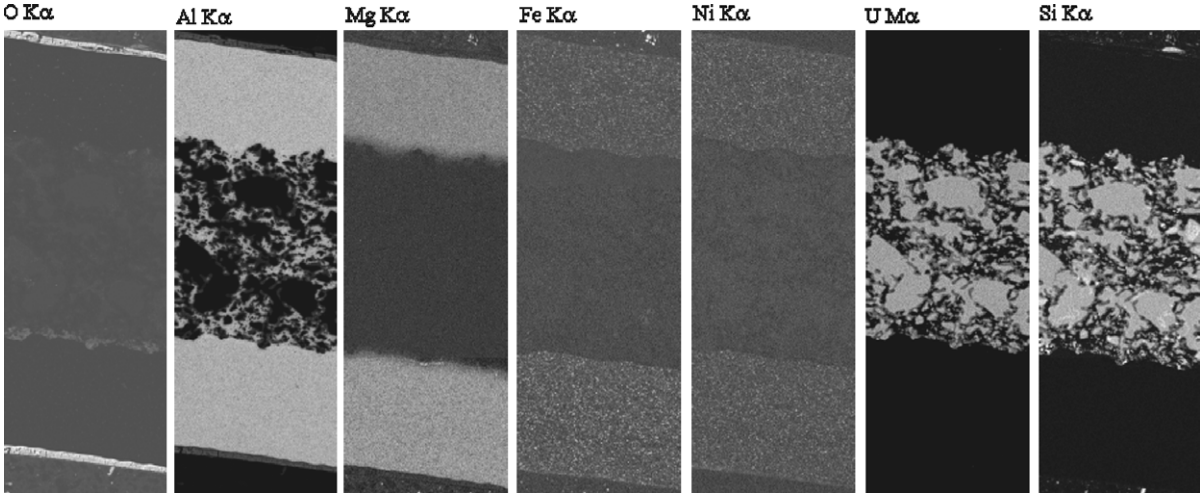

Fig. 7. O Kα, Al Kα, Mg Kα, Fe Kα, Ni Kα, U Mα and Si Kα X-ray maps showing the distribution of the elements over a complete section of the fuel plate.

zone, the Xe concentration is around 1.7 wt%, while in U_3Si_2 it drops to an average of 0.6 wt%. This lower value of xenon is due to precipitation of the gas in large bubbles. During sample preparation, some of these gas-filled bubbles get opened, the gas escapes and an apparent lower fission gas content will be measured. This effect is less severe for smaller bubbles. The Nd content, which remains in solid solution in U_3Si_2, is constant (average of 1.4 wt%) over the two zones.

The Xe X-ray image in Fig. 8 shows a lower concentration in the interaction layer and the formation of a halo of higher concentration around the particles. This phenomenon is related to the ejection of the fission products out of the grain and the sweeping of them during the growth of the Al–U–Si interaction layer [1]. Consequently, the fission products accumulate at the interface of the interaction layer and the matrix and as such produce a halo around the fuel particles. This is reflected in the quantitative linescan

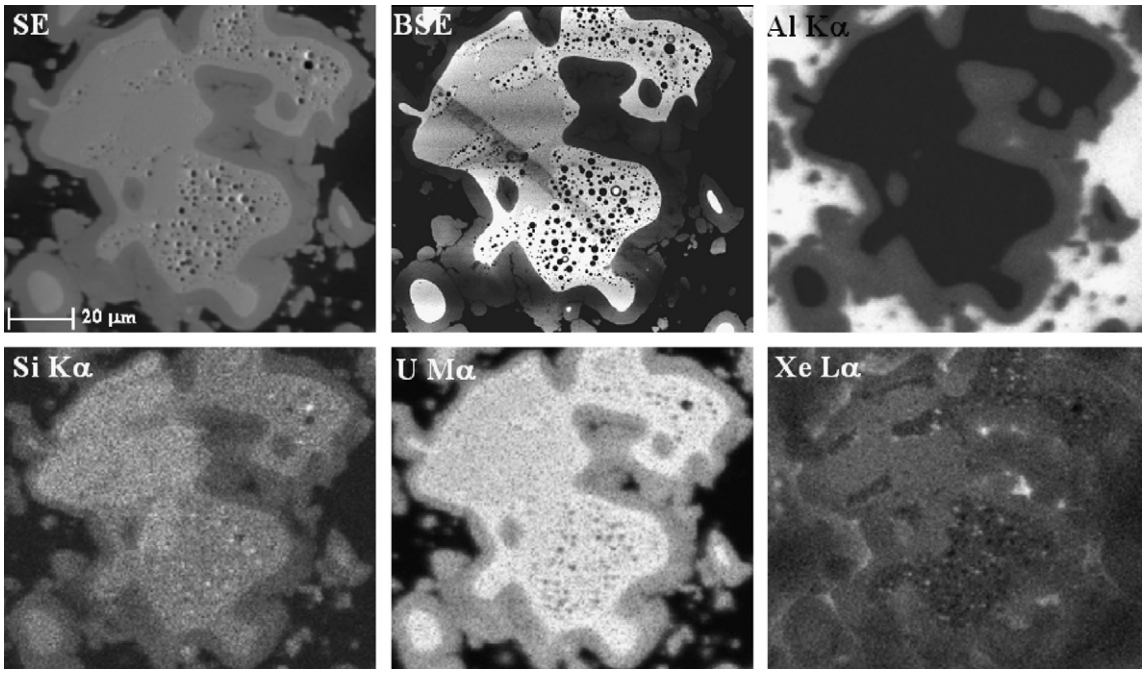

Fig. 8. Secondary electron (SE) image and local X-ray maps of respectively Al Kα, Si Kα, U Mα and Xe Lα of U_3Si_2 particles dispersed in the Al matrix. In the backscattered electron (BSE) image a contamination trace of the quantitative line scan analysis is seen.

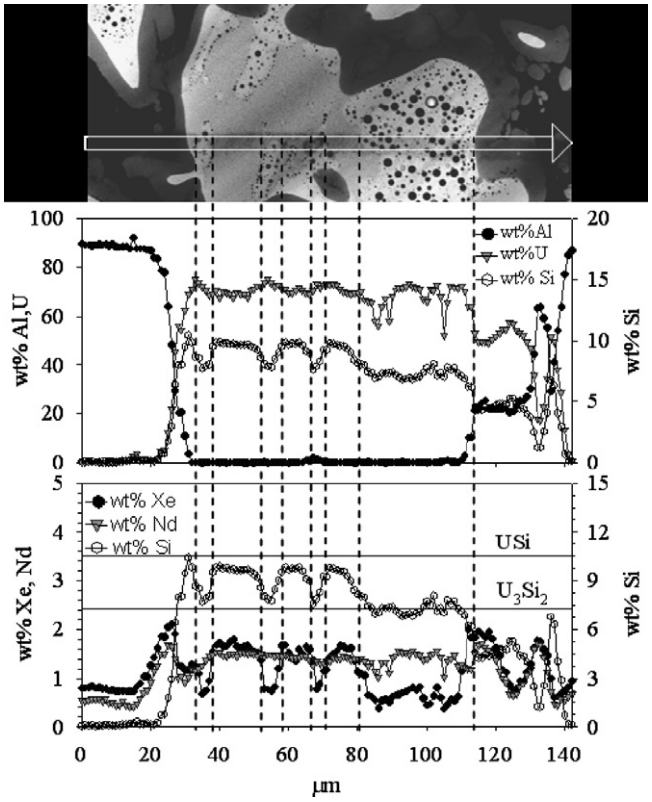

Fig. 9. Quantitative linescan over an inhomogeneous fuel particles. The boundaries of the areas containing either USi or U_3Si_2 are indicated by the vertical dashed lines.

data (Fig. 9) where a steep local rise of fission product concentrations can be seen at the interface of the interaction layer and the Al cladding.

The microhardness of the different phases in the meat has been measured and gives a Vickers hardness of HV290 for the fuel particles, HV408 for the U–Si–Al interaction layer and HV156 for the Al matrix.

4. Discussion

The three U_3Si_2 based fuel plates were successfully irradiated in the BR2 reactor and the non-destructive PIE showed no particularities.

During the irradiation, an oxide layer has formed on the outer AlFeNi cladding surfaces of the fuel plates. Lomakina et al. [4] found in a study on the corrosion of AlFeNi alloy in high-temperature water, that the thickness of the oxide film formed on the surface increases with increasing temperature. Electron microscopy studies showed that the hydrated oxide film is multilayered, consisting of an γ-aluminum layer attached to the metallic surface, a fine crystalline pseudoboehmite layer and finally a third layer consisting of large crystals with a boehmite structure. These observations are consistent with the current findings. From the eddy current measurement and the image analysis of the SEM images, it is found that the thickness of the layer is correlated to the heat flux profile over the plate width and hence the temperatures. XRD analysis shows that the oxide film consists of at least three distinct phases: aluminum, boehmite and bayerite. SE and BSE images (Figs. 3 and 5) also show a multilayered oxide film, the layer closest to the cladding containing AlFeNi precipitates, while in the other layer almost no particles are observed. The EPMA results also support the presence of two layers, with a varying aluminum content, but charging

of the non-conductive oxide layer prevents absolute quantification.

This double oxide layer is also observed by Kapusta and Wintergerst [6], in corrosion experiments on unirradiated AlFeNi cladding. The layer closest to the cladding, containing precipitates, is composed of mainly gibbsite or bayerite, while the outermost layer is boehmite. The assumed growth mechanism is a mixture of anionic and cationic diffusion.

The overall observation that the oxide layer is not firmly attached to the cladding and can easily be removed, leads to the assumption that dehydration of the layer must have occurred after the fuel element has been removed from the reactor, since there are no indications for in-pile exfoliation.

The main influence of the irradiation concerning the fuel meat, is the consumption of part of the Al matrix and the silicide fuel grains resulting in the formation of a U–Si–Al interaction phase.

In Fig. 10, the surface fractions occupied by the different phases found in the fuel plate are calculated by image analysis of micrographs recorded at several positions on the plate width. An increase of the fraction occupied by the U–Si–Al interaction layer, over the plate width is observed. The surface fraction occupied by the U_3Si_2 fuel particles decreases towards the fuel plate centre, but the even larger decrease in fraction taken up by the matrix is a good indication that the U–Si–Al interaction layer mainly grows at the expense of the Al matrix.

The interaction layer formed between the U_3Si_2 fuel and the Al matrix should have a composition intermediate between UAl_3 and USi_3 [7], two cubic compounds that are completely miscible [8], and lies on the tieline between Al and U_3Si_2 (Fig. 11). It is often reported as $U(Al,Si)_3$ with an Al to Si ratio of approximately 3.5 [7,9,10,11]. In the study of Marín et al. [12] a phase with a composition of 62 wt% U, 10.9 wt% Si and 26.8 wt% Al is misinterpreted as $U(Al,Si)_3$ as it should be $U(Al,Si)_{5.25}$. All previously mentioned (Al,Si) over U ratios are thermodynamically determined in out-of-pile studies. For the studies finding $U(Al,Si)_3$ [7,9,10] the annealing temperature was around 400 °C, while in the study of Marín et al. [12] finding a composition of $U(Al,Si)_{5.25}$ the annealing temperature was 610 °C.

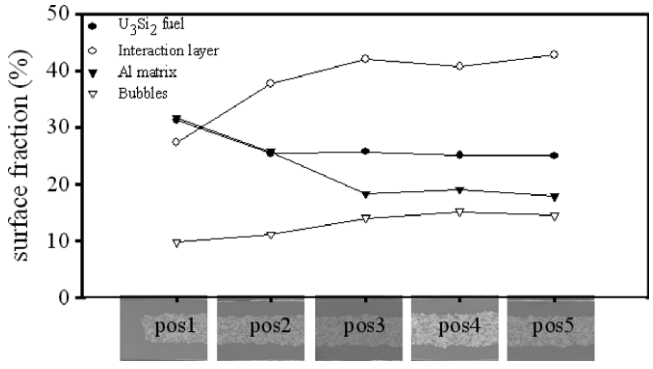

Fig. 10. Graphical representation of the surface fraction occupied by the fuel, Al–U–Si interaction layer, Al matrix and the fission gas-related bubbles, measured at several position over the width of the fuel plate (position 1 = side of the plate, position 4 = center of the plate).

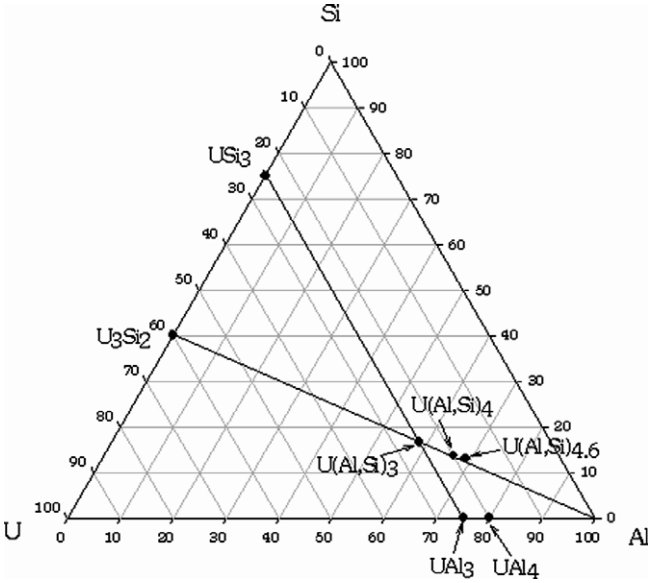

Fig. 11. Ternary Al–U–Si phase diagram. The formed interaction layer in the current study has a composition of $U(Al,Si)_{4.6}$.

The composition of the U–Si–Al interaction layer formed during an irradiation experiment is often described as $U(Al,Si)_3$ in reference to the out-of-pile experiments [7], but no results of actual measurements are reported in the open literature.

In the current study, it is found, based on averaging of several measurements, that the layer consists of 22.6 wt% Al, 4.7 wt% Si and 52.5 wt% U which results in a composition of $U(Al,Si)_{4.6}$ with an Al/Si ratio of 5. Taking into account that also the interaction layer will be depleted of uranium due to the burn-up, the composition would be intermediate between $U(Al,Si)_4$ and $U(Al,Si)_{4.6}$.

This inconsistency between out-of-pile and in-pile data is similar to the findings of Ryu et al. [13] in the U–Mo–Al system. Out-of-pile tests give Al/(U + Mo) ratios ranging between 3 and 4.4, while more Al rich phases with Al/(U + Mo) ratios of 3.3–7 are observed in in-pile experiments. The difference is explained by Ryu et al. that, at low irradiation temperatures, the interaction layer becomes amorphous. In this layer U, Mo and Al exist as a non equilibrium mixture. Due to fission-fragment damage inducing defects and disorder in the structure of the layer, a higher Al/(U + Mo) ratio than in the out-of-pile test is possible. Only if the irradiation temperature would increase substantially (above 400 °C), the crystalllinity would be restored and the Al/(U + Mo) ratio would decrease back to 3.

Since the irradiation temperature in the current described experiment stayed well below 400 °C, we can assume that the formed $U(Al,Si)_{4.6}$ interaction layer is indeed amorphous and as such can contain a high Al content.

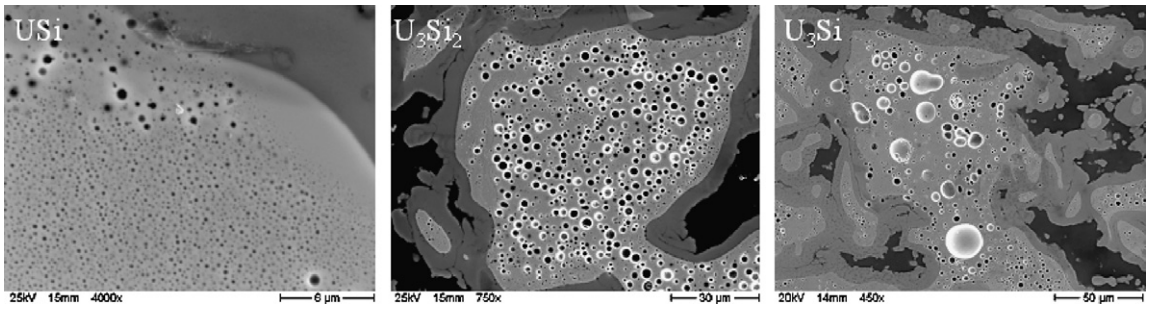

Fig. 12. Secondary electron image of fuel particles showing the differences in fission gas-related bubbles generated in the fuel phases USi, U_3Si_2 and U_3Si. Note the different magnification used for each of the images.

The amorphous character of the interaction layer formed in an U_3Si_2 fuel with a loading of 5.2 g/cm^3, irradiated up to 45% ^{235}U and 85% ^{235}U, characterised with neutron diffraction analysis is shown in [13]. Unfortunately the composition of the investigated interaction layer is not given.

The microscopy investigations on the fuel particles show that most of the fuel particles do not have a homogenous composition. Backscattered electron images show zones with different densities and the X-ray maps reveal zones with different Si enrichments, even within one particle. Quantification using EPMA demonstrate that the fuel is a mixture of U_3Si_2 and USi, and sporadically also a U_3Si particle is found. In practice, it is deemed to be nearly impossible to produce perfectly homogenous fuel [5,14]. The as-cast alloy usually contains particles consisting of U_3Si_2 and USi and some particles of U_3Si_2 and U_{SS} (uranium solid solution). Heat treating of the alloy will convert the U_{ss} in U_3Si, which is not a desirable phase as it is assumed to become amorphous when irradiated, resulting in breakaway swelling [15] in fuel plates. An excess of silicon is added to the alloy during the melting, to avoid the formation of large quantities of U_{SS} and hence U_3Si.

In the present case, the addition of excess Si effectively prevented the formation of large quantities of U_3Si (although some can be found), but resulted in the formation of important quantities of USi.

A considerable amount of fission gas-related bubbles have formed in the fuel. Detailed analysis of the SEM and BSE images in combination with the EPMA results, shows very clearly that the size of the bubbles is related to the composition of the fuel particles they are generated in. It is found that the fission gas bubbles in USi fuel are numerous and very small (100–300 nm) (Fig. 12(a)), while in the U_3Si_2 zones, the bubble diameter can be as large as a few micrometer, but fewer bubbles are found (Fig. 12(b)). It should be noted that all observed bubbles in USi and U_3Si_2 have a nearly perfectly round shape and no evidence of bubble coalescence is seen, indicating stable fission gas behaviour.

That the size of the fission gas bubbles is larger in the U_3Si_2 fuel than in the USi fuel is in contradiction with the observations made in [16,17], but in both references no adequate quantification is done of the phase of the observed fuel.

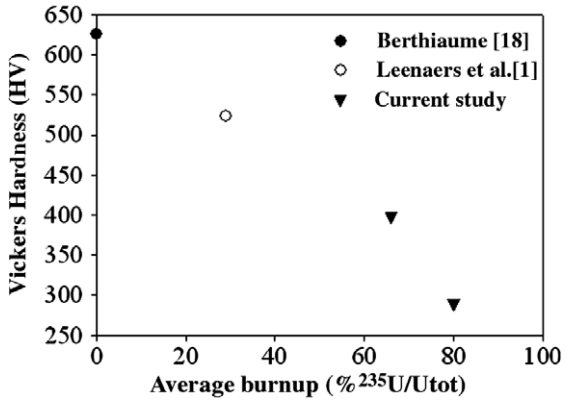

Fig. 13. Vickers hardness values found for U_3Si_2 fuel unirradiated and irradiated up to different burn-ups.

Some isolated particles having a U_3Si composition are also witnessed in the current study. These particles contain fission gas bubbles of varying shapes and sizes and signs of interlinkage are also observed (Fig. 12(c)).

In Fig. 11, the microhardness measurement in the fuel particles obtained in this study are compared to the results found in unirradiated U_3Si_2 fuel [18] and the measurement in the PIE campaign of the previous irradiation of U_3Si_2 fuel plates with an AG3-NET cladding [1]. To obtain an extra point in the graph, a second sample of the currently investigated fuel plate has been cut at a lower burn-up position (average of 66% $^{235}U/U_{tot}$) and prepared for microhardness measurements. From the graph (Fig. 13), it is seen that the U_3Si_2 fuel softens with increasing burn-up. A decrease in microhardness can be related to amorphisation of the fuel. The amorphisation of the U_3Si_2 fuel could give an explanation for the larger fission gas-related bubbles observed.

5. Conclusion

AlFeNi appears to be a good candidate cladding material for MTR dispersion fuel plates as an alternative to AG3-NET. The cladding behaved well under irradiation and no deterioration is observed apart from the formation of a multilayered oxide film. This oxide (hydroxide) forma-

tion and microstructural behaviour of AlFeNi in-pile appears to be very comparable to AG3-NET.

It has been observed that the oxide layer dries out when the plate is removed from the water, leading to cracking of the oxide layer which eventually leads to detachment but this behaviour is probably not exclusively related to AlFeNi. The oxide layer could be identified as a bayerite layer containing AlFeNi particles and a boehmite layer in which almost no precipitates is seen.

The fuel also behaved as expected under irradiation. A $U(Al,Si)_4$ interaction layer between the Al and the fuel particles has formed mostly at the expense of the Al matrix. But even after a (peak) burn-up of 87% ^{235}U, still ample of the Al matrix is left.

It has been observed and measured that the fuel particles are not homogenous in composition. It appears that most of them consist of a mixture of U_3Si_2 and USi. This compositional difference is reflected in the size of the fission gas-related bubbles. In USi the size of the bubbles is of the order of a few hundred nanometer, while in U_3Si_2 the bubble diameter can get as large as a few micrometer. Even with the inhomogeneity of the fuel, the overall performance of the fuel plates is very good.

References

[1] A. Leenaers, S. Van den Berghe, E. Koonen, P. Jacquet, C. Jarousse, B. Guigon, A. Ballagny, L. Sannen, J. Nucl. Mater. 327 (2004) 121.
[2] J.E. Hatch (Ed.), Aluminum: Properties and Physical Metallurgy, American Society for Metals, Metals Park, Ohio, 1983.
[3] R.E. Pawel, S.J. Pawel, Oak Ridge National Laboratory, report ORNL/M-4075 (1995).
[4] S.V. Lomakina, T.S. Shatova, L.P. Kazansky, Corr. Sci. 36 (1994) 1645.
[5] R.F. Domagala, in: proceedings of the 9th International Meeting on Reduced Enrichment for Research and Test Reactors (RERTR), Gatlinburg, Tennessee (1986).
[6] B. Kapusta, M. Wintergerst, (CEA, Saclay): Personal communication.
[7] G.L. Hofman, J. Rest, J.L. Snelgrove, T. Wiencek, in: proceedings of the 19th International Meeting on Reduced Enrichment for Research and Test Reactors (RERTR), Seoul, Korea (1996).
[8] A.E. Dwight, Argonne National Laboratory Report No. ANL-82-14, Argonne, IL (1982).
[9] K.-H. Kim, J.-M. Park, C.-K. Kim, G.L. Hofman, K.-W. Paik, J. Nucl. Mater. 270 (1999) 315.
[10] M. Ugajin, M. Akabori, A. Itoh, N. Ooka, Y. Nakakura, J. Nucl. Mater. 248 (1997) 204.
[11] P. Toft, A. Jensen, in: proceedings of the 8th International Meeting on Reduced Enrichment for Research and Test Reactors (RERTR), Petten, The Netherlands (1985).
[12] J. Marín, J. Lisboa, J. Ureta, L. Olivares, H. Contreras, J.C. Chávez, J. Nucl. Mater. 228 (1996) 61.
[13] H.J. Ryu, Y.S. Kim, G.L. Hofman, D.D. Keiser, in: proceedings of the 28th International Meeting on Reduced Enrichment for Research and Test Reactors (RERTR), Cape Town, South Africa (2006).
[14] Office of Nuclear Reactor Regulation, report NUREG-1313 (1988).
[15] M.R. Finlay, G.L. Hofman, J. Rest, J.L. Snelgrove, in: proceedings of the 24th International Meeting on Reduced Enrichment for Research and Test Reactors (RERTR), San Carlos de Bariloche, Argentina (2002).
[16] M.R. Finlay, G.L. Hofman, J.L. Snelgrove, J. Nucl. Mater. 325 (2004) 118.
[17] G. Ruggirello, H. Calabroni, M. Sanchez, G.L. Hofman, in: proceedings of the 24th International Meeting on Reduced Enrichment for Research and Test Reactors (RERTR), San Carlos de Bariloche, Argentina (2002).
[18] L.C. Berthiaume, Atomic Energy of Canada Limited, report AECL-3517 (1969).